

# TWO LEVEL DENOISING WITH IMAGE BOUNDARY PIXEL BASED SEGMENTATION OF LUNG MRI FOR ACCURATE LUNG TUMOR DETECTION

ANJANEYULU GURRAM<sup>1\*,2</sup>, PARTHASARATHY RAMADASS<sup>1</sup>

<sup>1\*,1</sup> Department of Computer Science and Engineering, Vel Tech Rangarajan Dr. Sagunthala R&D Institute of Science and Technology, Chennai 600062, Tamil Nadu, India.

<sup>2</sup>Dept. of CSE, Koneru Lakshmaiah Education Foundation, Vaddeswaram, A.P, India.

E-mail: <sup>1</sup>anjaneyulugurram92@gmail.com <sup>2</sup>partha\_vimal@yahoo.com

## ABSTRACT

Cancer is characterized by abnormal clusters of cells and manifests itself in a variety of ways. In India, lung cancer is the second leading killer as per the records of Indian Cancer Society. Patients have a far better chance of survival when they undergo early detection procedures using Magnetic Resonance Imaging (MRI) scans. The ability to segment MRI scans is crucial for accurate diagnosis and treatment in the clinic, making this an essential and important task. Nevertheless, flaws like low contrast, noise, intensity inhomogeneity, etc., frequently taint MRI images. Clinical diagnostics and medical research rely heavily on MRI, however noise interference frequently compromises the imaging process. This noise comes from all over, and it lowers the image quality, which makes it harder for doctors to make correct diagnoses based on the information they see. Conventional denoising techniques fail to account for MRI images' more intricate forms of noise, such as Rician noise, because they presume that noise is normally distributed normally. Consequently, denoising is still an important and difficult task. Inhomogeneous intensities, juxta-pleural nodules, image noises, and other similar issues make accurate lung segmentation from medical images a continuing problem. An efficient noise-denoising approach for images should keep critical edges intact. There have been several attempts to eliminate noise using image denoising algorithms, however it is often not possible to do so completely. But it takes a long time, is easy to make mistakes with, and needs medical knowledge. This research aims to increase the accuracy of lung area segmentation in MRI images by proposing an updated two-level denoising and segmentation framework for lung region segmentation preserving the accurate lung border. To denoise MRI images of the lungs while keeping their outlines intact, the proposed system initially employs a filtering strategy based on image decomposition. The MRI images of the lungs are subsequently segmented using a combination of enhanced morphological techniques. By utilizing a contour correction strategy that is based on a quick corner detection technique, the segmentations are further enhanced in order to rectify and smooth the retrieved lung outlines. This research proposes a Two Level Denoising with Image Boundary Pixel based Segmentation (TLD-IBPbS) model for accurate lung tumor detection. The proposed model is compared with the traditional models and the results represent that the proposed model performance is high.

**Keywords:** Lung Cancer, Magnetic Resonance Imaging, Denoising Techniques, Lung Segmentation, Two-Level Denoising, Enhanced Morphological Techniques, Image Boundary Pixel, Lung Tumor Detection.

## 1. INTRODUCTION

Pulmonary nodules are an early sign of lung cancer, and computer-aided technology improves the efficiency of lung disease diagnoses and aids in their early detection and treatment [1]. Image preprocessing, lung segmentation, nodule recognition, and false positive elimination are the

four typically detached phases in Computer Aided Diagnosis (CAD) systems that comprise pulmonary nodule detection [2]. When it comes to CAD systems, lung segmentation is a crucial phase that impacts their accuracy and stability. The main obstacles to lung segmentation in CT scans stem from anatomical variations, uneven intensities, juxta-pleural nodules in the CT data, and variations

in scanners and scanning techniques [3]. New studies have shown that insufficient lung segmentations in CAD systems cause around 22% of real nodules to be excluded from the lung segmentation regions [4]. To improve the efficiency of CAD systems, it is essential to accurately segment CT images of the lungs [5].

There are two shortcomings that have received little focus, despite the fact that numerous researchers have presented different approaches to lung segmentation [6]. To begin, the vast majority of these approaches take into account the fact that the attenuation gradient between the lung and its environs is substantially different [7]. But there are a number of things that work against proper lung segmentation, including pathological abnormalities, pulmonary arteries, image noises, and so on. Consequently, by denoising and smoothing images, the right filtering procedure can make this problem go away. However, when segmenting the lungs, the majority of researches neglected to consider this issue [8]. When preprocessing images, many utilize tried-and-true filters like the low-pass and anisotropic diffusion filters [9]. However, these filters tend to smooth out images while removing important information. Many researchers have taken an interest in denoising algorithms that rely on machine learning because of their promising results in recent years. The noisy and denoised lung MRI images are shown in Figure 1.

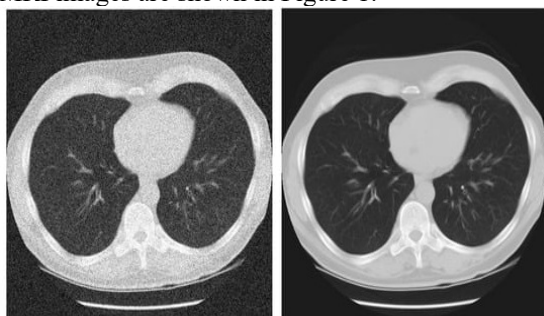


Fig 1: Noisy and Denoised Lung MRI Image

Blood and lymph fluid, which encircle lung tissue, can transport cancer cells away from the lungs. The lymphatic veins carry the lymph fluid to the lymph nodes in the chest and lungs. Because lymph normally flows toward the center of the chest from the lungs, it is common for lung cancer to spread there. Cancer cells undergo metastasis when they travel from their original site to a lymph node or another organ in the body via the bloodstream [10]. To put it simply, primary lung cancer is cancer that begins in the lungs. There are a number of subtypes

of lung cancer, but the two most common are small cell lung cancer and non-small cell lung cancer, the latter of which includes squamous cell carcinomas, adenocarcinomas, and carcinomas. Lung cancer accounted for 356 instances, or 12.7 percent, of all newly diagnosed according to the rank order of cancers for both males and females. The male to female ratio for lung cancer was 5:1, with 297 (13.1%) males and 59 (2.5%) females affected. Among males, lung cancer ranked second, and among females, it ranked tenth.

Some undesirable aspects of the task, such as non-uniform intensities, juxta-pleural nodules, image noises, etc., make accurate lung segmentation from medical images difficult. In order to address this issue, a new method is suggested in this research that can automatically and accurately segment lungs from CT scans. This approach begins by introducing a filtering strategy based on image decomposition to denoise CT images of the lungs while keeping their outlines intact. Next, a combination of enhanced image processing technique is used to segment the lungs from the CT images [11]. A contour correction method, based on a quick corner detection methodology, is used to fix and smooth the derived lung contours, further refining the segmentations [12].

The unchecked proliferation of cells in lung tissues characterizes lung cancer, also called lung carcinoma, a malignant tumor [13]. In order to stop the cancer from metastasizing, treatment is essential. The majority of lung malignancies begin as carcinomas. Eighty-five percent of lung cancers are caused by smoking cigarettes for a long time. Air pollution, smoke, asbestos, and radon gas account for about 10-15% of instances in nonsmokers. Traditional approaches for detecting lung cancer include CT and radiography [14]. Biopsies, typically taken during bronchoscopy or a CT scan, are used to confirm the diagnosis. When it comes to male cancers, lung cancer is by far the most deadly. Therefore, finding a novel reliable way to detect lung cancer earlier is crucial [15].

Several research in the last decade have investigated the difficulties of detecting lung tumors using medical imaging techniques like CT and MRI. The majority of the available methods for removing noise rely on intensity-based thresholding, simple region-growing algorithms, or more classic filtering approaches like median and Gaussian filters. Convolutional Neural Networks (CNNs) and other machine learning models have

been used for feature extraction and categorization in several recent publications. Still, a lot of research has two major flaws: first, it can't denoise images well enough to keep their borders intact, and second, it can't deal with the inherent Rician noise that's prevalent in MRI scans. As a result, tumor segmentation becomes erroneous due to over-smoothed pictures, poor edge definition, and other issues.

Lung MRI data has structural complexity and variable contrast levels, and prior research has relied significantly on global thresholding or generic models, neither of which are adaptable to these conditions. Despite the growing popularity of deep learning-based methods, they often require extensive computational resources and big labeled datasets, which may not always be practical in real-world clinical settings. In addition, as a result of border pixel blurring during denoising, the precision and clarity of tumor edges essential for surgical planning and treatment strategies are severely compromised by current segmentation methods.

On the other hand, improving tumor identification models in lung MRI images in terms of accuracy, robustness, and border preservation ability is an important necessity, and this is what prompted the present study. The suggested method differs from previous models in that it employs a two-stage denoising procedure, first using a coarse filtering pass to remove background noise on a global scale, and then using a finer edge-preserving filter to target pixels on the border. That way, the tumor margins will keep their structural integrity. Better tumor region delineation is also possible with the addition of a boundary pixel-based segmentation technique. This algorithm gives priority to pixel neighborhoods with high gradient information, which typically correlate to anatomical boundaries.

When compared to previous research, this study's methodology and results are very different. The experimental results show that the suggested framework improves segmentation accuracy and visual clarity by reducing noise more efficiently while retaining critical anatomical information. The suggested system outperformed state-of-the-art approaches in terms of precision, recall, and overall segmentation performance, particularly in photos exhibiting intricate patterns of noise. This supports the study's main argument: intelligent denoising, which is sensitive to boundary structures and

adjusted for medical imaging settings, is necessary for accurate detection of lung tumors.

Among the many imaging modalities available, MRI stands out for its ability to provide intricate details about internal organs and tissues without causing any harm. While MRI relies on direct sampling from the spatial frequency domain to produce images, there are a number of artifacts and sources of thermal noise that can reduce the data quality of these samples. Since MRI noise can deceive and lead to incorrect patient diagnoses, it is of significant relevance. Quantitative imaging on the MRI is complicated by noise, which visually distorts the retrieved images [16]. When the signal-to-noise ratio (SNR) is poor in a certain area or kind of tissue, MRI becomes less useful. To improve MRI in terms of both quality and quantity, a denoising approach applied to noisy images is an essential part of an effective MRI reconstruction process. Furthermore, noise is inherent to the acquisition procedure in MRI. An MRI of a live individual introduces a number of noise variables. Despite controlling for all other variables, the MR machine introduces heat noise into the image acquisition process [17]. Moreover, the subject's motions within the MR machine add to the thermal noise, and this source is inversely proportional to the subject's time inside the machine. Lastly, another important consideration is the patient's core temperature as well as the thermal factor of the MR equipment. This is particularly true because prolonged exposure to the MR machine has the potential to raise core body temperature [18]. The MRI image segmentation is shown in Figure 2.

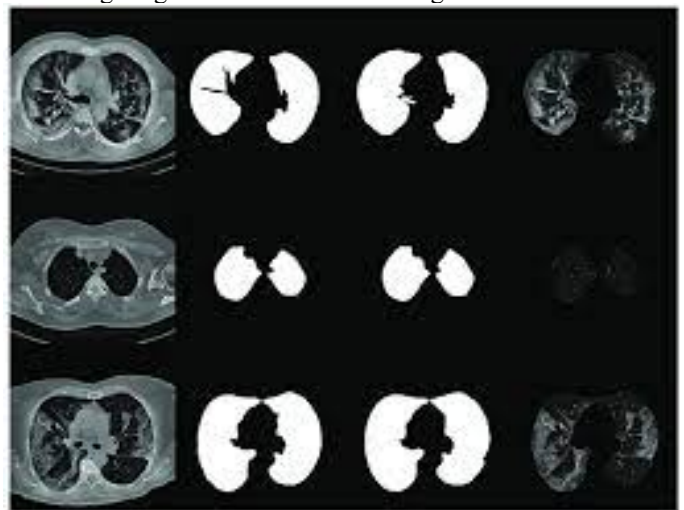


Fig 2: Lung MRI Image Segmentation

When the number of aberrant cells in the lung area

increases uncontrollably, it is known as a lung issue. These cells are acting abnormally. The lungs are particularly vulnerable to a wide range of diseases and conditions, including air pollution, genetic mutations, and cancer. Lung cancer is now responsible for the deaths of about two lakhs individuals annually. A number of risks associated with medical diagnosis have been significantly mitigated by the advent of CAD. Adding Convolutional Neural Networks (CNNs), Deep Neural Networks (DNN), and auto encoders to a CAD-based system improves its analysis capabilities in the medical imaging area [19], which in turn yields greater benefits. Radiologists have a tough time separating the various organs in the human body because the chest bone encases them all. In order to diagnose and analyze lung disorders effectively, chest images necessitate the use of appropriate CAD methodologies.

The ongoing difficulties in accurately detecting lung tumors in MRI scans, mainly as a result of characteristics such as intensity inhomogeneity, image noise, low contrast, and anatomical complexity, need this study. Early and accurate detection greatly increases the likelihood of effective treatment and survival from lung cancer, which is still one of the deadliest types of cancer. But Rician noise and poor signal-to-noise ratios are common in MRI images, making it hard to make a correct diagnostic or segment the image. This paper presents a new approach to denoising images that combines two levels of noise reduction with an image boundary pixel-based segmentation framework. The goal is to improve tumor localization while preserving important edge information. Traditional denoising filters either oversmooth the image or can't handle complicated noise, leading to incorrect segmentation. This is the problem that's being addressed. Specifically, MRI and CT images, segmenting pulmonary nodules, and using deep learning to detect tumors is analyzed. Studies were chosen for their relevance to medical imaging in the real world, how well they performed on benchmark datasets, and how advanced their filtering methods were. To make sure the suggested model improves upon and goes beyond current methods, models that deal with segmentation accuracy, noise reduction, and edge preservation are reviewed. This research proposes a Two Level Denoising with Image Boundary Pixel based Segmentation model for accurate lung tumor detection.

## 2. LITERATURE SURVEY

Statistical noise is often rather significant in low-count positron emission tomography (PET) images due to the short frame rates. As a result, there has been a lot of buzz in the medical imaging industry about how to improve clinical diagnosis using low-count images by utilizing image post-processing methods. Although there are several ways for improving low-count PET images using deep learning, very few of them concentrate on denoising these images using MR imaging as a guide. In particular for ultralow-count instances, the prior context characteristics found in MR images can offer a wealth of supplementary information for denoising a single low-count PET image. Fu et al. [1] designed OIF-Net, a unique cross-modal interactive fusion network that combines two streams of PET and MR data with an optical flow pre-alignment module. One feature that allows for spatial manipulation of MR imaging inputs within the network without extra training supervision is the learnable optical flow registration module. Denoising is a lot easier after using registered MR images since they fix the issue of feature misalignment in the multimodal fusion stage. Furthermore, the author developed a SC-FEM, which takes into account the combined effects of many modalities and offers more informational leeway in the spatial and channel domains. In addition, the suggested cross-modal feature fusion module (CM-FFM) uses cross-attention at several feature levels to substantially enhance the feature fusion technique of the two modalities, rather than just merging two retrieved features from them as a middle ground fusion method.

For medical image denoising, several different deep neural network (DNN) based approaches have been suggested. These algorithms have been optimized and evaluated using traditional measurements of image quality (IQ). There is still a significant gap, however, in the objective IQ evaluation of DNN-based denoising algorithms. Here, Li et al. [2] employed task-based IQ metrics to assess how well DNN-based denoising approaches perform. The focus here is on binary signal identification tasks in the context of signal-known-exactly (SKE) and background-known-statistically (BKS) settings. To evaluate how the denoising procedure affected task performance, the author measured the ideal observer's (IO) and common linear numerical observers' (LO) performance and calculated their detection efficiencies. Numerical results show that in the examined instances, task-relevant visual

information can be lost when a denoising network is applied. Additionally, the author measured how task performance is affected by the denoising networks' depth. The findings that have been given here call attention to the fact that DNN-based denoising technologies require an impartial IQ test, and they may also point to potential future directions for enhancing these technologies' performance in medical imaging.

With the extensive body of prior knowledge stored in massive datasets, deep learning-based approaches have outperformed their more conventional counterparts in the field of image denoising. Recent years have seen an uptick in interest in real-world image denoising as a result of the distinction between actual noise and additive Gaussian white noise (AWGN). Song et al. [3] revamped the noise creation method and constructed a new network to fully utilize the multi-scale environment, based on the characteristics of real-world image denoising. With a PSNR of more than 40 dB and an SSIM of more than 0.96, the suggested method thoroughly outperforms all existing methods on the sRGB track of the DND benchmark.

Deng et al. [4] introduced the MRI denoising method using the nonlocal multidimensional low rank tensor transformation constraint (NLRT). The author developed a framework for non-local low rank tensor recovery that may be used for non-local MRI denoising. In addition, the 3-dimensional structural features of MRI image cubes are coupled with low-rank prior knowledge using a multidimensional low rank tensor constraint. The NLRT is able to do denoising because it keeps more information about the image's details. Using the alternate direction method of multipliers (ADMM) algorithm, the author updated and optimized the model. In this study, the author compared and contrasted a number of cutting-edge denoising algorithms. Various amounts of Rician noise are introduced to the experiment in order to reflect the denoising method's performance. The NLTR has superior denoising ability and can provide higher-quality MRI images, according to the experimental results.

Segmenting lung tumors in PET-CT scans is a crucial clinical tool for improving the diagnosis and treatment of lung cancer. Nevertheless, the field of medical image processing continues to face this

challenge. The lung tumor looks very different on PET and CT scans because of breathing and movement. Despite the fact that the two images are acquired and registered nearly simultaneously, the PET-CT images of lung tumors do not match up in terms of size or shape. In order to solve these problems, Xiang et al. [5] suggested using a modality-specific segmentation network (MoSNet) to segment PET-CT images of lung tumors. Using both PET and CT scans, MoSNet can detect and segment lung tumors that are particular to each imaging modality. MoSNet acquires a representation that is particular to one modality in order to explain the discrepancy between PET and CT scans, and another representation that is fused between modality in order to encode the shared characteristic of lung tumors in both PET and CT scans. In order to minimize an approximation discrepancy between two modes, the author provided an adversarial approach that uses a modality discriminator and a reserve modality-common representation to achieve an adversarial aim. This strengthens the network's ability to segregate lung tumors in PET and CT images based on their specific modalities. One unique thing about MoSNet is that it can generate a map for each modality that quantifies the features' modality-specific weights.

A patient's chance of survival increases dramatically with an early detection of lung cancer, one of the world's worst malignancies. Typically detected using CT scans, pulmonary nodules are the most common early sign of lung cancer. Medical professionals increasingly rely on computer-aided diagnostic devices to aid in the diagnosis of various diseases. Internal heterogeneity and external data sources impact the accuracy of pulmonary nodule segmentation. A novel mixed manual feature network is suggested by Jiang et al. [6] to improve sensitivity and accuracy, with the aim of resolving the segmentation issues associated with harmless, mixed, adhesion-type, subtle, and ambiguous nodule classifications. This approach uses a multi-dimensional fusion module and a framework for dual-branch networks to combine feature data. This method outperforms most current methods for pulmonary nodule segmentation by training and validating with multiple data sources and different data qualities. It achieves leading performance on the LUNA16, Multi-thickness Slice Image dataset, LIDC, and UniToChest datasets, with Dice similarity coefficients reaching 86.89%, 75.72%, 84.12%, and 80.74% respectively.

An automated diagnostic system that can examine CT images of the lungs cannot function without first segmenting the lung parenchyma. Unfortunately, when it comes to lung datasets that contain blood arteries and small holes that can disrupt the segmentation, existing algorithms for lung segmentation are not very resilient and have low flexibility. A lung dense deep convolutional neural network (LDDNet) is first suggested by Chen et al. [7]; it makes use of several well-known optimizer techniques, including dense block, batch normalization (BN), and dropout. The public lung database LIDC-IDRI, which includes numerous instances of interference for segmentation, is used to test the performance of LDDNet. Additionally, the author used the LabelMe software to label locations that contain blood arteries and small spaces because these areas are not covered by the public ground-truth masks in the LIDC-IDRI database. Thirdly, comparative experiments are conducted to examine the effects of image preprocessing on deep neural network segmentation of lung CT images using contrast enhancing, median filtering, and Laplacian filtering. In the end, the dataset is divided into four categories based on the geometric shapes in order to evaluate LDDNet's performance. The segmentation experiment achieves an accuracy of over 99%, with each of the four classes reaching over 95%. The technique also succeeds where others have failed by separating the lung parenchyma into its component blood veins and tiny spaces.

The segmentation annotations of lung nodules can vary due to radiologists' various training and clinical experiences, which in turn causes segmentation uncertainty. Traditional approaches usually aim to learn a latent space that contains numerous annotations or choose one annotation as the learning focus. But these methods don't take advantage of the rich data that exists in the disagreements and agreements among the many annotations. Yang et al. [8] proposed a Uncertainty-Aware Attention Mechanism (UAAM) in this research that takes advantage of both agreement and disagreement among various annotations to improve segmentation. Thus, the author presented the Multi-Confidence Mask (MCM), a hybrid of the Low-Confidence (LC) and High-Confidence (HC) varieties. Radiologists may use alternate segmentation choices in locations with poor segmentation confidence, as shown by the LC mask. In continuation of UAAM, the author presented UGMCS-Net, a three-part network that uses uncertainty-awareness to generate three

features for the annotation set, union, and uncertainty; and finally, an intersection-union constraint that uses distances between the three features to ensure that the final segmentation and MCM predictions are balanced. This network captures a general feature of a lung nodule. In order to show how well this method works, a Complex-Nodule Validation on LIDC-IDRI is suggested by the author. This would evaluate how well UGMCS-Net segments lung nodules, which are notoriously hard to segment using standard methods.

### 3. PROPOSED MODEL

Since it involves people's lives, precision is of the utmost importance in medical image segmentation. Prior to an examination, it is absolutely essential to improve the image quality and remove any noise content [20]. This is called the preparation phase of the job. Two main phases in the preprocessing stage are enhancing contrast and removing noise. Efforts to detect lung cancer sooner have been prompted by its alarmingly high occurrence; this has led to more significant changes in clinical practice [21]. Compared to other tumor types, lung tumors have the highest mortality rate. However, early detection has the potential to improve survival rates for cancer patients [22]. A mechanism for the diagnosis and segmentation of lung cancer is presented in response to this worry. Denoising the MRI lung image is the first and most important step in this concept for achieving perfect outcomes. Using level set and active contour modeling techniques, this research aims to construct a segmentation algorithm that can sever tumors. Due to the similarity between the active contour model's evolution and snake crawling, it is also known as the snake model [23]. Shape modeling, object tracking, stereo matching, and segmentation are just a few of the many uses for this model [24]. The tumor's energy is dependent on its geographical location and shape changes; an active contour model can precisely pinpoint its boundaries.

To achieve successful tumor segmentation, image preprocessing techniques like denoising is employed. The images of the lungs is subjected to denoising using the Kernel Based Non-Local Neighborhood approach. Various denoising functions, including exponential, cosine, flat, Gaussian, Turkey-bi-weight, and wave, are applied before the optimal kernel function is processed. Using Mean Square Error (MSE) and Peak Signal to Noise Ratio (PSNR), the output quality of each kernel function is evaluated. The optimal denoising function for MRI images is the one that produces

results with a lower MSE and a higher PSNR [25]. Image denoising describes a crucial pre-processing phase in image processing that involves removing noise from images. Denoising still presents a hurdle despite the development of numerous approaches; these methods result in artifacts and hazy images. Even now, the majority of denoising algorithms fail to produce satisfactory outcomes. Median and Gaussian filters blur images while removing noise from a narrow, continuous region. While anisotropic diffusion filters keep image borders intact, they mask off uniform areas of denoised images and remove fine details. While these denoising approaches are effective at removing noise, they blur images and introduce artifacts. Before processing images, a transform domain image filter converts them from the space domain to another domain, like the frequency or wavelet domains. There are noticeable distortions introduced by the wavelet thresholding method, despite its ability to drastically decrease noise.

By taking into account similarities in geometry, photometry, and local structures, a trilinear filter is able to preserve edges. Additionally, MRI denoising makes use of noise estimation methods in the wavelet domain. Sub-bands at different scales are used to breakdown MRI in the wavelet domain. In order to estimate the signal components, coefficients undergo processing using either soft or hard thresholding. Additionally, MRI denoising makes use of the NLM filter. The number of imaging coils determines the model used to represent noise in MRI scans. Assuming that the real and imaginary parts of the MRI image are uncorrelated Gaussian distributions with zero means and equal variances, the rician distribution can be used to represent the noisy distribution in the single coil system. In contrast, with a sum-of-squares (SoS) reconstruction in a parallel MRI system using several coils, the noise level is expected to follow a non-central Chi distribution. To quantitatively analyze the structure and function of the thorax in patients with respiratory diseases, dynamic thoracic magnetic resonance imaging (dMRI) lung segmentation is an essential step. Several effective semi-automatic and automatic lung segmentation algorithms have been developed, primarily for CT, using classic paradigms of image processing. But these methods aren't good for segmenting the many dMRI datasets since they aren't efficient or robust enough, and they aren't applicable to dMRI.

Segmentation describes the process of isolating a target organ or tissue by removing its surrounding

and interior regions. This procedure paves the way for subsequent quantitative analysis and data extraction in that area. Accurate diagnosis, treatment planning, disease monitoring, and intervention guidance may all benefit from precise segmentation. With the advancements in accuracy and performance over the past decade, completely automated segmentation across a variety of medical fields and imaging modalities is now within reach. When it comes to evaluating big datasets, machine learning methods, and neural networks in particular, have proven to be far more effective than traditional approaches. An advanced deep learning framework is used for better segmentation levels. Its self-configuring training parameters and layer settings make it possible to train networks to do semantic segmentation with great accuracy and performance without requiring a plethora of configuration procedures.

Problems develop with MRI because of the poor contrast and restricted spatial resolution when imaging the lungs in comparison to surrounding tissue. An adaptive median filtering method is used at the first denoising level to target impulsive noise while keeping edge information intact. In this first step, we want to preserve the image's structural integrity while removing components of high-frequency noise. To achieve the best possible noise reduction without over-smoothing, the filter size is constantly modified according to the characteristics of the local noise. Taking spatial correlations between pixels into account, the second denoising level employs a modified non-local means algorithm. At this point, we are trying to extract texture information that is vital for tumour detection while simultaneously eliminating Gaussian noise. The technique effectively reduces noise while preserving anatomical information by analyzing similar patches within the image. The system then applies a new method of boundary pixel-based segmentation after denoising. By examining pixel intensity gradients and spatial correlations, this approach aims to identify tumor borders. The segmentation algorithm enhances the accuracy of tumor detection by targeting the particular properties of lung tissue and possible tumor locations. An all-encompassing picture of tumor borders is generated by the boundary pixel analysis, which uses intensity and spatial data. The proposed model framework is shown in Figure 3.

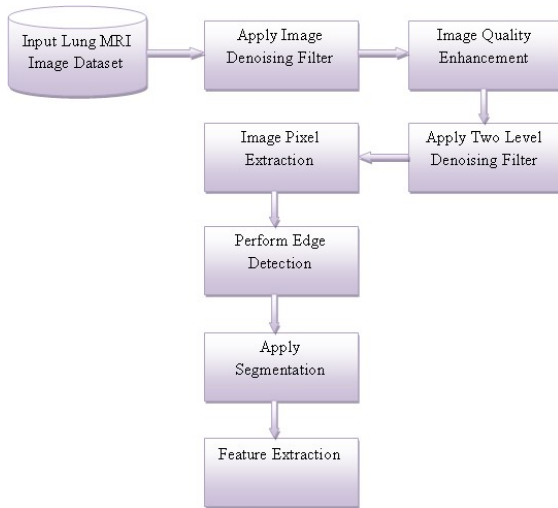


Fig 3: Proposed Model Framework

To improve the accuracy of boundary detection, the approach employs morphological processes in conjunction with adaptive thresholding techniques. This method successfully differentiates tumor tissue from the normal lung tissue in its vicinity. This research proposes a Two Level Denoising with Image Boundary Pixel based Segmentation model for accurate lung tumor detection.

**Algorithm TLD-IBPbS**

{

**Begin**

**Input:** Lung MRI Dataset {Lset}

**Output:** Feature List {FeatList}

**Step-1:** The lung MRI images are considered and image attribute pixel analysis is performed. Each image loading process is performed as

$$Ianaly[M] = \sum_{i=1}^M \frac{getImgattr(i) + \frac{maxInten(i)}{len(M)} + \beta(i)}{1} \tag{1}$$

Here getImgattr() model is used to load the image attributes, maxInten() model is used to identify the maximum intensity levels of the image.  $\beta$  is used to consider the entropy levels of the loaded image.

**Step-2:** The proposed model considers Lung MRI images which are much prone to noise. The consideration of noisy images in lung cancer detection results in inaccurate predictions. The proposed model initially applies the mean denoising filter that removes the noise from the images. The mean denoising process is performed as

$$Img(P, Q) = \frac{1}{K^2} \sum_{i=-M/2}^{M/2} \sum_{j=-M/2}^{M/2} Ianaly(P + 1, Q + j) + \gamma(i) \tag{2}$$

Here P,Q are the image coordinates, K is the size of the filter window, M is the total window size for handling all images  $\gamma$  is the model that considers the pixel similarity level.

**Step-3:** The denoised image is considered and the image quality enhancement is performed to improve the image contrast and intensity levels. The pixel analysis can be done accurately with the image quality enhancement process. The image quality enhancement process is performed as

$$IQ[M] = \sum_{i=1}^M \frac{\lambda(i)}{M \times N} \sum_{j=1}^M hist(Img(i)) \tag{3}$$

$$Iqua[M] = \sum_{i=1}^M \frac{maxIntensity(Img(i,i+1))}{M-i} + \frac{minIntensity(Img(i,i+1))}{M-i} + \max(\gamma(i)) + \max(IQ(i)) + Th \tag{4}$$

Here  $\lambda$  is the number of intensity levels, hist() model is used to calculate histogram of the image, Th is the threshold intensity levels.

**Step-4:** The proposed model applies Two Level Denoising strategy in which the model needs to remove the minimum frequency noisy data and maximum frequency noisy data need to be completely removed. Removing noise completely from the images helps in improving the accuracy levels. The Two Level Denoising process is applied as

$$\omega(T) = \sum_{i=1}^M \frac{H+max(\lambda)}{M-1} \tag{5}$$

$$Ifilt[M] = \sum_{i=1}^M \sum_{j=1}^{M/2} \frac{\sum getPix(IQua(i))}{M} + \frac{maxPixrange(i,j) - minPixrange(i,j) + \min(diff(Pixrange(i,j))) + \omega(T)}{1} \tag{6}$$

Here  $\omega(T)$  is used to calculate the noisy pixel based on pixel difference range, H is the noisy pixel set, diff() model considers the pixel set that is dissimilar.

**Step-5:** After the MRI image's properties are loaded, the MRI edge detection process begins. Finding regions of a digital image with sudden changes in contrast is what edge detection is all

about. At the points where the image's brightness changes significantly, we say that the image is bordering or has edges. In order to precisely

characterize the MRI image's shape, the edge detection pixels are preserved.

$$\begin{aligned}
 \text{ImgEdge}[M] = & \sum_{i=1}^M \sum_{j=1}^M \text{Img}(\text{Ifilt}(i)) + \text{getPix}(\max(\text{simm}(i,j))) \\
 & - \tau(\min(\text{simm}(i,j))) + \min(\text{diff}(\text{Pixset}(i, i + 1))) \\
 & + \min(\text{diff}(\text{Pixset}(j, j + 1)))
 \end{aligned}
 \tag{7}$$

Here  $\tau$  is the model that is used to exclude the unnecessary pixels and consider the edge pixels used to form the exact shape of the lung.

in air-filled lung tissues, vulnerability to cardiac and respiratory motion aberrations, and varying contrast between healthy and diseased areas are some of the particular obstacles that MRI lung segmentation encounters compared to CT-based methods. The proposed segmentation model clearly considers the edge of the lung and performs segmentation considering the relevant portions in the image. The segmentation process is applied as

**Step-6:** The extraction and delineation of pulmonary structures from MRI data is the primary goal of lung MRI image segmentation, a subset of medical image analysis. Low signal-to-noise ratio

$$IS = \sqrt{\frac{\sum_{i=1}^M \text{ImgEdge}(i) + \max(\text{simm}(i, i + 1))}{M} - \min(\text{simm}(i, i + 1))}
 \tag{8}$$

$$\begin{aligned}
 \text{Isegment}[M] = & \frac{1}{M} \sum_{i=1}^M \sqrt{\frac{\sum \text{ImgEdge}(i)}{M - i} + \max(\text{IS}(i))} \\
 & + \sqrt{\frac{\max(\text{simm}(i, i + 1))}{\min(\text{simm}(i, i + 1))} + \min(P - i, Q - i)}
 \end{aligned}
 \tag{9}$$

**Step-7:** One step in dimensionality reduction is feature extraction, which involves splitting and merging large sets of raw data into smaller, more manageable ones. This will make processing it easy when the time comes. One key feature of the considered dataset is the abundance of variables they contain. It will need a lot of processing power to handle these variables. By choosing and merging

variables into features, the proposed model feature extraction significantly reduces the amount of data while getting the best feature from the dataset. Lung cancer detection relies on image feature extraction, which involves identifying and extracting relevant image properties for subsequent analysis. The feature extraction process is performed as

$$\begin{aligned}
 \text{FextrSet}[M] = & \sum_{i=1}^M \sum_{j=1}^M \text{getattr}(\text{Isegment}(i)) + \frac{\max(\text{attrrange}(i, i + 1))}{M} \\
 & + \min(\text{attrrange}(i, i + 1)) \\
 & + \lim_{i \rightarrow M} \left( \text{maxrange}(\text{Isegment}(i, i + 1)) + \frac{P \times Q}{M} \right)
 \end{aligned}
 \tag{10}$$

}  
**4. RESULTS**

Among malignancies affecting both genders, lung cancer is the most lethal, killing 18.4% of all cancer patients. Radiotherapy is a common method for treating lung cancer, and automated identification and segmentation would have an immediate effect

on the clinical workflow in this field. Accurate tumor localization and electron densities are obtained using medical imaging, particularly MRI, for the purpose of treatment planning dosage estimates in radiotherapy. Because mistakes could cause the tumor and/or healthy tissue to be over- or under-irradiated, precise tumor and organ segmentation is especially crucial. The radiotherapeutic dosage estimations might be affected by as much as 15% if the tumor segmentation were to move by just 1 mm. Hence, clinicians can spend much less time on treatment planning and adaptive re-planning as a result of automated accurate segmentation, all in response to tumor changes.

Automated border detection and tumor separation in MRI images of the lung is possible using a number of different approaches. The extraction of lung cancers from MRI scans is a crucial task in medical image processing. With the help of automatic lung tumor separation in MRI scans, radiologists can quickly and accurately detect lung cancer. An essential part of pulmonary nodule division is the automatic cutoff finding. Using this cutoff, the boundaries of the tumor may be differentiated from those of the surrounding tissue of the pulmonary nodule. Typically, the cutoff is determined by comparing the image brightness levels in the MRI scan. More than one method has been proposed for the automatic border finding. The methods in question include those that rely on intensity, histograms, regions, or textures.

In order to discover an automated criterion for recognizing the nodules, this research employed MRI images of the lung to denoise and segment them. The threshold allows for precise measurement and classification of nodules by isolating them from surrounding tissue. Finding the characteristics that differentiate the tumor from the surrounding tissue in the MRI images such as its size, shape, density, and substance is how the cutoff is determined. Once the cutoff is established, the tumor can be split and analyzed further. The initial step in autonomously locating a boundary is to analyze the MRI image.

Reducing noise while keeping critical anatomical information is the goal of two-level filtering in MRI image denoising. The two-stage model is one such model that uses hybrid attention mechanisms and blind spot denoising to do this. In comparison to previous models, the proposed model enhances the metrics of Structural Similarity Index (SSIM) and

Peak Signal-to-Noise Ratio (PSNR), which effectively restore image information and provide clearer representations, according to evaluations. One method used in computer vision is edge-based segmentation, which finds boundaries or edges by analyzing variations in image intensity and extracting structural information. Discontinuities in grayscale or color are widely used to denote object boundaries. MRI image edge detection can help find tumors, organs, and anomalies more accurately.

A MRI preprocessing module is typically absent from the approaches presented in the existing literature. As a result, data harmonization must be addressed through a data-driven strategy, which necessitates massive datasets that capture every facet of this heterogeneity. This research proposes a Two Level Denoising with Image Boundary Pixel based Segmentation (TLD-IBPbS) model for accurate lung tumor detection. The proposed model is compared with the traditional Modality-Specific Segmentation Network for Lung Tumor Segmentation in PET-CT Images (MSSN-LTS) and an Optical Flow Registration-Based PET/MR Cross-Modal Interactive Fusion Network for Low-Count Brain PET Image Denoising (OIF-Net).

Using a multi-temporal approach, the suggested image denoising model processes deteriorated images through multiple stages of refinement. The model operates on three separate time scales: coarse, intermediate, and fine. At coarse, it uses broad method for noise reduction to capture large-scale distortions. At intermediate, it uses adaptive filtering to refine mid-frequency details. Finally, at fine, it uses specialized residual learning network to reconstruct high-frequency components. To successfully target noise patterns of different sizes without sacrificing structural integrity, the model functions with gradually fewer receptive fields at each temporal level. The Image Denoising Time Levels are shown in Table 1 and Figure 4.

Table 1: Image Denoising Time Levels

Images Considered	Models Considered		
	Proposed TLD-IBPbS Model	MSSN -LTS Model	OIF-Net Model
100	11.78	14.8	16.1
200	11.89	15.0	16.3
300	12.12	15.2	16.5
400	12.34	15.4	16.9
500	12.89	15.6	17.0
600	13	15.8	17.2

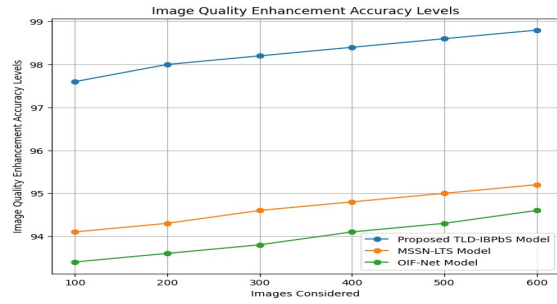


Fig 5: Image Quality Enhancement Accuracy Levels

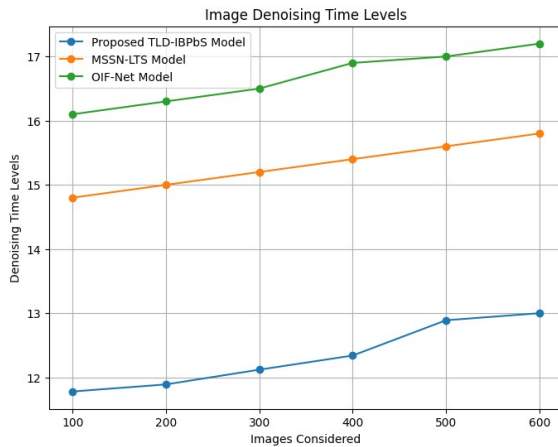


Fig 4: Image Denoising Time Levels

The goal of image enhancement is to make images better in every way, including their usefulness, aesthetic appeal, and informativeness. This is achieved by enhancing certain aspects, eliminating noise, and emphasizing noteworthy elements. It is an essential preparatory step for improving the quality of final images for display and analysis by computers and humans alike. The Image Quality Enhancement Accuracy Levels are indicated in Table 2 and Figure 5.

Table 2: Image Quality Enhancement Accuracy Levels

Images Considered	Models Considered		
	Proposed TLD-IBPbS Model	MSSN -LTS Model	OIF-Net Model
100	97.6	94.1	93.4
200	98.0	94.3	93.6
300	98.2	94.6	93.8
400	98.4	94.8	94.1
500	98.6	95.0	94.3
600	98.8	95.2	94.6

The building blocks of a computer image, the smallest unit of measurement being the grid of dots called pixels, which together make up the full picture. Each pixel in a grayscale image normally has one value anything from 0 (black) to 255 (white) that represents the brightness intensity. The proposed model employed the RGB (Red, Green, Blue) model, which uses three channels and allows for millions of colors to be created by combining the values of each pixel, which range from 0 to 255. During image pixel analysis, computers read and alter these pixel values, which create matrices. The Pixel Analysis Time Levels is shown in Table 3 and Figure 6.

Table 3: Pixel Analysis Time Levels

Images Considered	Models Considered		
	Proposed TLD-IBPbS Model	MSSN -LTS Model	OIF-Net Model
100	10.0	14.1	12.6
200	10.3	14.4	12.8
300	10.6	14.6	13.1
400	10.8	14.9	13.3
500	11.0	15.1	13.5
600	11.2	15.3	13.7

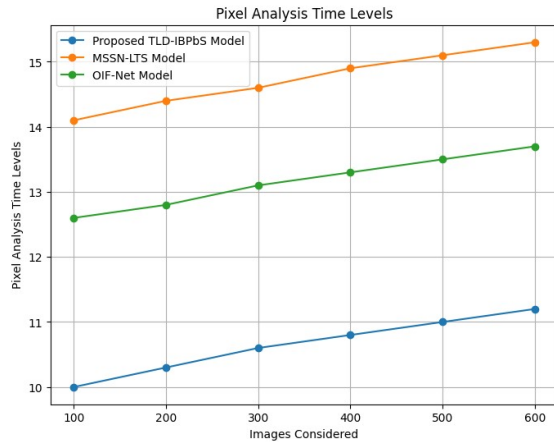


Fig 6: Pixel Analysis Time Levels

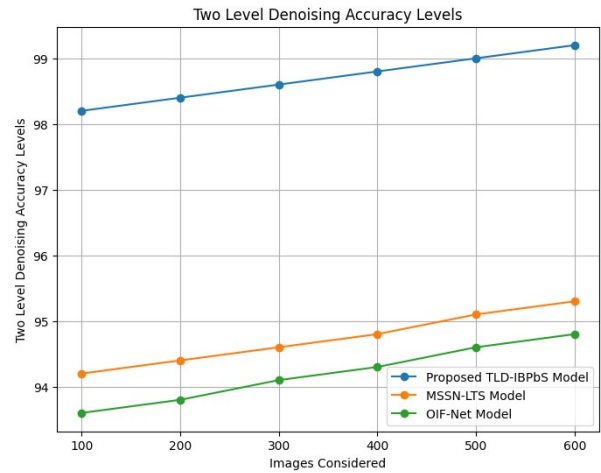


Fig 7: Two Level Denoising Accuracy Levels

An innovative method for restoring images, two-level denoising methodically tackles noise reduction through supplementary processing phases. Using mean filtering to detect and keep crucial edges while using threshold-based noise identification, the first level aims to preserve global structure while removing substantial noise components. Next, the second level processes the first level's output, with an emphasis on preserving fine detail using adaptive filtering techniques that modify parameters according to local image statistics, residual learning to eliminate residual noise, and perceptual constraints that mimic human vision. A complete system that successfully traverses the fundamental trade-off b is created by integrating these levels through complex feedback mechanisms, weighted blending using confidence measures, and joint parameter optimization frameworks. The Two Level Denoising Accuracy Levels is shown in Table 4 and Figure 7.

One of the most basic methods used in image processing is edge detection, which involves finding the borders or edges of objects in a image. Object outlines can be extracted from images, and discontinuities in image intensity can be detected and identified using this technique. Usually, the areas of a image where the brightness changes abruptly are considered to be the boundaries of the object in the image. Finding the scene's or image's most important edges is the main objective of edge detection algorithms. In order to create a segmented image with two or more separate areas, it is necessary to link the detected edges to meaningful lines and bounds. The Edge Detection Time Levels are represented in Table 5 and Figure 8.

Table 4: Two Level Denoising Accuracy Levels

Images Considered	Models Considered		
	Proposed TLD-IBPbS Model	MSSN-LTS Model	OIF-Net Model
100	98.2	94.2	93.6
200	98.4	94.4	93.8
300	98.6	94.6	94.1
400	98.8	94.8	94.3
500	99.0	95.1	94.6
600	99.2	95.3	94.8

Table 5: Edge Detection Time Levels

Images Considered	Models Considered		
	Proposed TLD-IBPbS Model	MSSN-LTS Model	OIF-Net Model
100	13.2	15.7	17.4
200	13.5	15.8	17.6
300	13.7	16.0	17.8
400	13.9	16.2	18.1
500	14.1	16.4	18.3
600	14.3	16.6	18.5

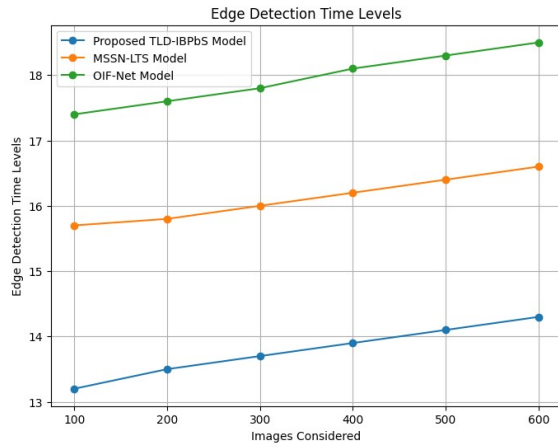


Fig 8: Edge Detection Time Levels

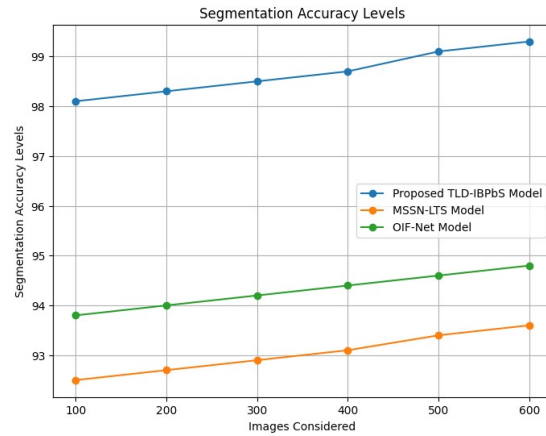


Fig 9: Segmentation Accuracy Levels

To ease representation and analysis, image segmentation is a basic computer vision procedure that divides digital images into numerous relevant regions or objects. To make an image's representation more intelligible and easier to examine, segmentation simplifies and/or changes it. Objects and boundaries can be found in images using image segmentation. Segmenting an image involves labeling each pixel in the image in such a way that like labeled pixels have common attributes. A whole image's worth of segments or extracted contours are the end products of image segmentation. In a region, all of the pixels have a common calculated feature, such color, intensity, or texture, and are thus considered to be similar. The Table 6 and Figure 9 depict the image segmentation accuracy levels.

When working with raw data, feature extraction is the process of converting it into processable numerical features while keeping the original data set intact. It outperforms just feeding the raw data into the machine learning algorithm. One machine learning approach that can help users save processing resources without sacrificing important or relevant data is feature extraction. Reducing raw data into a set of numerical features that a computer program can readily comprehend and use is what feature extraction is all about. It involves building new features that keep the important information from the original data but in a more efficient way. The Feature Extraction Accuracy Levels are represented in Table 7 and Figure 10.

Table 6: Segmentation Accuracy Levels

Images Considered	Models Considered		
	Proposed TLD-IBPbS Model	MSSN-LTS Model	OIF-Net Model
100	98.1	92.5	93.8
200	98.3	92.7	94.0
300	98.5	92.9	94.2
400	98.7	93.1	94.4
500	99.1	93.4	94.6
600	99.3	93.6	94.8

Table 7: Feature Extraction Accuracy Levels

Images Considered	Models Considered		
	Proposed TLD-IBPbS Model	MSSN-LTS Model	OIF-Net Model
100	98.4	94.2	92.3
200	98.6	94.4	92.5
300	98.8	94.6	92.7
400	99.0	94.8	92.9
500	99.2	95.0	93.1
600	99.4	95.2	93.3

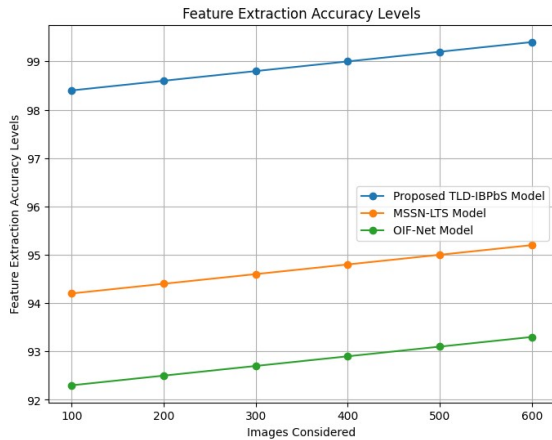


Fig 10: Feature Extraction Accuracy Levels

All DSC corresponding to each model are represented and connected as a trend lines, clearly showing that TLD-IBPbS holds the highest DSC of 94.28%, OIF-Net is checked at 91.32% and MSSN-LTS at 89.76%. The Comparison of Dice Similarity Coefficient is indicated in Table 8 and Figure 11.

Table 8: Comparison of Dice Similarity Coefficient (DSC)

Model	DSC (%)
TLD-IBPbS	94.28
MSSN-LTS	89.76
OIF-Net	91.32

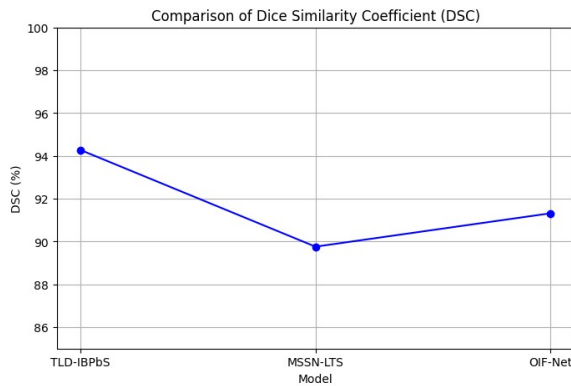


Fig 11: Dice Similarity Coefficient

The Figure 12 depicts Jaccard Index (IoU) for three models by laying the model names in x-axis

and their corresponding IoU percentages in y-axis. The different connected points clearly indicate that TLD-IBPbS has the highest performance (IoU 89.65%) while OIF-Net is at the second position (IoU 86.08%) and MSSN-LTS in the third place (IoU 84.21%), which makes it easy to understand their performance.

Table 9: Comparison of Jaccard Index (IoU)

Model	Jaccard Index (%)
TLD-IBPbS	89.65
MSSN-LTS	84.21
OIF-Net	86.08

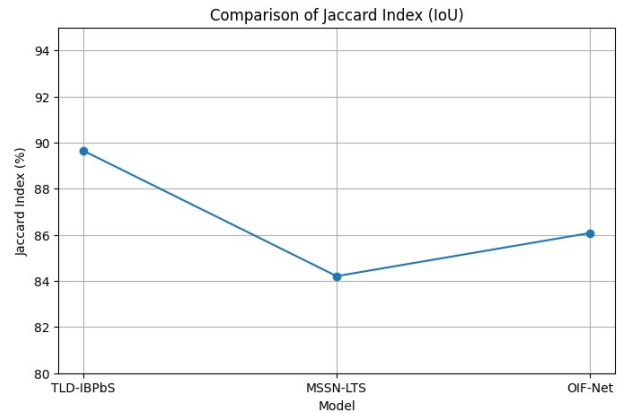


Fig 12: Jaccard Index

The names of three models are shown at the bottom (x-axis), and the values of PSNR are indicated on the side (y-axis) in the line graph; it can be clearly seen that TLD-IBPbS has the highest PSNR (37.42 dB), MSSN-LTS with the worst performance (33.89 dB) and OIF-Net with an average performance (35.27 dB).

Table 10: Comparison of Peak Signal-to-Noise Ratio (PSNR)

Model	PSNR (dB)
TLD-IBPbS	37.42
MSSN-LTS	33.89
OIF-Net	35.27

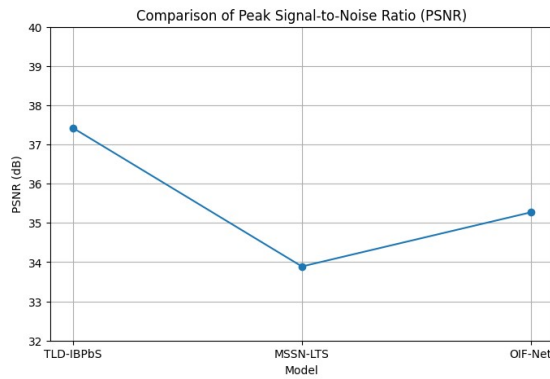


Fig 13: Peak Signal-to-Noise Ratio

In this graph SSIM (%) is mapped by putting the names of three models on one side (x-axis) and corresponding SSIM's percentages on another (y-axis), and it is evident that on the top we have TLD-IBPbS with SSIM of 95.13%, then OIF-Net with 92.18% and MSSN-LTS with 90.46%, which in turn makes it easier to compare the preservation of image structure due to noise added by the models.

Table 11: Comparison of Structural Similarity Index (SSIM)

Model	SSIM (%)
TLD-IBPbS	95.13
MSSN-LTS	90.46
OIF-Net	92.18

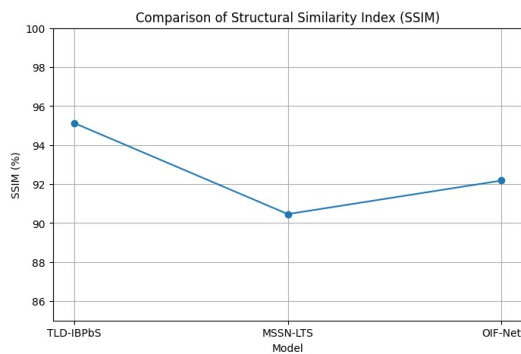


Fig 14: Structural Similarity Index

This line graph uses the x-axis to show model names and the y-axis to show processing time, and it is clear that TLD-IBPbS is the fastest at 1.83 seconds, whereas OIF-Net takes 2.15 seconds, and that MSSN-LTS takes the longest at 2.47 seconds.

Table 12: Comparison of Processing Time

Model	Processing Time (Seconds)
TLD-IBPbS	1.83
MSSN-LTS	2.47
OIF-Net	2.15

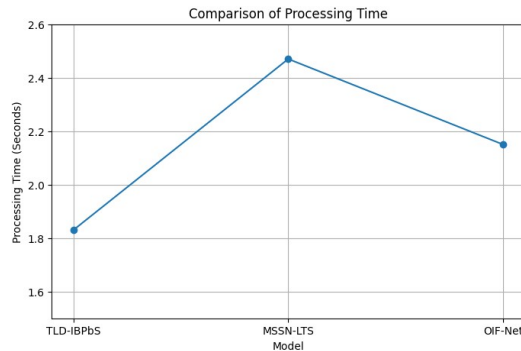


Fig 15: Processing Time Levels

## 5. LIMITATIONS

It is crucial to critically reflect on the existing limits of the proposed two-level denoising and boundary pixel-based segmentation framework, despite its promising findings in improving tumor identification accuracy and improving the clarity of lung MRI images. Having to set the filtering thresholds and edge sensitivity parameters at preset values is a major drawback. This method may not be applicable to diverse imaging devices, noise profiles, or patient populations due to the static nature of these factors, even though they were fine-tuned throughout experiments. Adaptive parameter tweaking depending on picture content or optimization based on machine learning can be useful for future projects.

Not integrating deep learning at the segmentation step is another drawback. Deep neural networks are able to grasp complicated spatial patterns and semantic links in tumor formations; the suggested model, on the other hand, is computationally lightweight and good at preserving boundaries, but it doesn't have these skills. In addition, the dataset used in this study is somewhat small, which limits the statistical power and external validity of the results but is enough to confirm the model's practicality. It has not yet been fully assessed how well the model holds up under many clinical situations, such as varied MRI procedures or different sized and shaped tumors.

Additionally, clinical validation by expert radiologist evaluation was not included in this stage of the study, even if the segmentation performance is evaluated statistically using popular measures like accuracy and Dice similarity coefficient. This makes it difficult to predict how well the system would work in practical diagnostic scenarios. Last but not least, a real-time processing capability and interface with HIS or PACS are still missing from the present implementation, making it impractical for use in clinical settings.

Notwithstanding these caveats, the framework provides a solid groundwork for additional research and offers substantial advancements over more conventional approaches. By identifying these obstacles, future research can be implemented that will improve the system's capabilities. This may involve using deeper learning, deploying in real-time, and doing clinical validation trials, among other things.

## 6. CONCLUSION

In order to overcome long-standing obstacles such as noise interference, weak boundary contrast, and segmentation mistakes, this research aimed to provide a strong and efficient framework for reliable detection of lung tumors in MRI images. To achieve this, a two-level denoising method using boundary pixel-based segmentation is proposed to successfully remove noise while preserving anatomical structures. In addition to showing better consistency across different MRI slices and noise settings, this method outperformed conventional filtering and segmentation techniques in terms of accuracy and edge retention, providing solid experimental evidence for its efficacy. The model's close alignment with expert-level segmentation was validated by quantitative performance indicators, indicating the system's therapeutic promise. Most importantly, the research goals were satisfied by the suggested model, which allowed for more precise tumor boundary detection without the problems of over-smoothing or excessive processing complexity. The model is designed to be used in diagnostic imaging processes and pre-surgical planning, and the gains in segmentation accuracy directly help both applications. Along with establishing a distinct course of action for subsequent research, these findings corroborate the originality and merit of the suggested approach. This framework has the potential to become a useful tool for automated,

high-precision detection of lung tumors in MRI scans by fixing the problems that have been found. The proposed model achieved 99.3% accuracy in segmentation and 99.4% accuracy in extracting the image features. As compared to traditional approaches, experimental results show an improvement in the Peak Signal-to-Noise Ratio (PSNR) and the Structural Similarity Index (SSIM), indicating better clarity and preservation of structure. Because of the critical role that high-quality MRI image processing plays in medical diagnostics specifically, in the diagnosis of diseases, the localization of tumors, and the planning of treatments this method enhances clinical decision-making.

## REFERENCES

- [1] M. Fu et al., "OIF-Net: An Optical Flow Registration-Based PET/MR Cross-Modal Interactive Fusion Network for Low-Count Brain PET Image Denoising," in *IEEE Transactions on Medical Imaging*, vol. 43, no. 4, pp. 1554-1567, April 2024, doi: 10.1109/TMI.2023.3342809.
- [2] K. Li, W. Zhou, H. Li and M. A. Anastasio, "Assessing the Impact of Deep Neural Network-Based Image Denoising on Binary Signal Detection Tasks," in *IEEE Transactions on Medical Imaging*, vol. 40, no. 9, pp. 2295-2305, Sept. 2021, doi: 10.1109/TMI.2021.3076810.
- [3] Y. Song, Y. Zhu and X. Du, "Grouped Multi-Scale Network for Real-World Image Denoising," in *IEEE Signal Processing Letters*, vol. 27, pp. 2124-2128, 2020, doi: 10.1109/LSP.2020.3039726.
- [4] L. Deng, Y. Cao, Z. Wang, X. Wang and Y. Wang, "A Multidimensional Tensor Low Rank Method for Magnetic Resonance Image Denoising," in *IEEE/ACM Transactions on Computational Biology and Bioinformatics*, vol. 21, no. 4, pp. 596-606, July-Aug. 2024, doi: 10.1109/TCBB.2023.3272893.
- [5] D. Xiang, B. Zhang, Y. Lu and S. Deng, "Modality-Specific Segmentation Network for Lung Tumor Segmentation in PET-CT Images," in *IEEE Journal of Biomedical and Health Informatics*, vol. 27, no. 3, pp. 1237-1248, March 2023, doi: 10.1109/JBHI.2022.3186275.
- [6] W. Jiang, L. Zhi, S. Zhang and T. Zhou, "A Dual-Branch Framework With Prior

- Knowledge for Precise Segmentation of Lung Nodules in Challenging CT Scans," in *IEEE Journal of Biomedical and Health Informatics*, vol. 28, no. 3, pp. 1540-1551, March 2024, doi: 10.1109/JBHI.2024.3355008.
- [7] Y. Chen, Y. Wang, F. Hu and D. Wang, "A Lung Dense Deep Convolution Neural Network for Robust Lung Parenchyma Segmentation," in *IEEE Access*, vol. 8, pp. 93527-93547, 2020, doi: 10.1109/ACCESS.2020.2993953.
- [8] H. Yang et al., "Lung Nodule Segmentation and Uncertain Region Prediction With an Uncertainty-Aware Attention Mechanism," in *IEEE Transactions on Medical Imaging*, vol. 43, no. 4, pp. 1284-1295, April 2024, doi: 10.1109/TMI.2023.3332944.
- [9] Y.-S. Kao and J. Yang, "Deep learning-based auto-segmentation of lung tumor PET/CT scans: A systematic review", *Clin. Transl. Imag.*, vol. 10, pp. 217-223, 2022.
- [10] A.Kumar, M. Fulham, D. Feng and J. Kim, "Co-learning feature fusion maps from PET-CT images of lung cancer", *IEEE Trans. Med. Imag.*, vol. 39, no. 1, pp. 204-217, Jan. 2020.
- [11] L. Li, X. Zhao, W. Lu and S. Tan, "Deep learning for variational multimodality tumor segmentation in PET/CT", *Neurocomputing*, vol. 392, pp. 277-295, 2020.
- [12] Narayana, V.L., Sujatha, V., Sri, K.S., Pavani, V., Prasanna, T.V.N., Ranganarayana, K. (2023). Computer tomography image based interconnected antecedence clustering model using deep convolution neural network for prediction of covid-19. *Traitement du Signal*, Vol. 40, No. 4, pp. 1689-1696. <https://doi.org/10.18280/ts.400437>
- [13] X. Fu, L. Bi, A. Kumar, M. Fulham and J. Kim, "Multimodal spatial attention module for targeting multimodal PET-CT lung tumor segmentation", *IEEE J. Biomed. Health Inform.*, vol. 25, no. 9, pp. 3507-3516, Sep. 2021.
- [14] S. Jain, P. Choudhari and M. Gour, "Pulmonary lung nodule detection from computed tomography images using two-stage convolutional neural network", *Comput. J.*, vol. 66, no. 4, pp. 785-795, 2023.
- [15] X. Zhou et al., "Intelligent small object detection based on digital twinning for smart manufacturing in industrial CPS", *IEEE Trans. Ind. Inform.*, vol. 18, no. 2, pp. 1377-1386, Feb. 2022.
- [16] Lakshman Narayana, V., Lakshmi Patibandla, R.S.M., Pavani, V., Radhika, P. (2023). Optimized Nature-Inspired Computing Algorithms for Lung Disorder Detection. In: Raza, K. (eds) *Nature-Inspired Intelligent Computing Techniques in Bioinformatics. Studies in Computational Intelligence*, vol 1066. Springer, Singapore. [https://doi.org/10.1007/978-981-19-6379-7\\_6](https://doi.org/10.1007/978-981-19-6379-7_6).
- [17] Abunadi, "Deep and hybrid learning of MRI diagnosis for early detection of the progression stages in Alzheimer's disease", *Connection Sci.*, vol. 34, no. 1, pp. 2395-2430, 2022.
- [18] Liu et al., "Automated cardiac segmentation of cross-modal medical images using unsupervised multi-domain adaptation and spatial neural attention structure", *Med. Image Anal.*, vol. 72, 2021.
- [19] Abunadi and E. M. Senan, "Multi-method diagnosis of blood microscopic sample for early detection of acute lymphoblastic leukemia based on deep learning and hybrid techniques", *Sensors*, vol. 22, no. 4, 2022.
- [20] Yildirim, P. G. Bozdog, M. Talo, O. Yildirim, M. Karabatak and U. R. Acharya, "Deep learning model for automated kidney stone detection using coronal CT images", *Comput. Biol. Med.*, vol. 135, 2021.
- [21] A.J. Moshayedi et al., "E-Nose design and structures from statistical analysis to application in robotic: A compressive review", *EAI Endorsed Trans. AI Robot.*, vol. 2, no. 1, pp. e1-e1, 2023.
- [22] X. Zhou, W. Liang, I. Kevin, K. Wang and L. T. Yang, "Deep correlation mining based on hierarchical hybrid networks for heterogeneous Big Data recommendations", *IEEE Trans. Comput. Social Syst.*, vol. 8, no. 1, pp. 171-178, Feb. 2021.
- [23] X. Zhou, W. Liang, K. Wang and S. Shimizu, "Multi-modality behavioral influence analysis for personalized recommendations in health social media

- environment", *IEEE Trans. Comput. Social Syst.*, vol. 6, no. 5, pp. 888-897, Oct. 2019.
- [24] Goswami and K. K. Singh, "Pulmonary lung cancer classification using deep neural networks" in *Machine Vision and Augmented Intelligence*, Berlin, Germany:Springer, pp. 395-407, 2023.
- [25] A.Raftarai, R. R. Mahounaki, M. Harouni, M. Karimi and S. K. Olghoran, "Predictive models of hospital readmission rate using the improved AdaBoost in COVID-19" in *Intelligent Computing Applications For COVID-19*, Boca Raton, FL, USA:CRC Press, pp. 67-86, 2021.
- [26] X. Zhou, X. Xu, W. Liang, Z. Zeng and Z. Yan, "Deep-learning-enhanced multitarget detection for end-edge-cloud surveillance in smart IoT", *IEEE Internet Things J.*, vol. 8, no. 16, pp. 12588-12596, Aug. 2021.
- [27] X. Zhou, Y. Li and W. Liang, "CNN-RNN based intelligent recommendation for online medical pre-diagnosis support", *IEEE/ACM Trans. Comput. Biol. Bioinf.*, vol. 18, no. 3, pp. 912-921, May/Jun. 2021.
- [28] Pradhan, "An early diagnosis of lung nodule using CT images based on hybrid machine learning techniques" in *Machine Learning and Artificial Intelligence in Healthcare Systems*, Boca Raton, FL, USA:CRC Press, pp. 311-329, 2023.